

The Quefrency Alanysis of Time Series for Echoes: Cepstrum, Pseudo-Autocovariance, Cross-Cepstrum and Saphe Cracking

Bruce P. Bogert
M. J. R. Healy
John W. Tukey

1. INTRODUCTION

The use of the power spectrum and other techniques based on Fourier analysis has proved exceedingly powerful in work on time series arising in many different fields of research. The problems dealt with were

The Collected Works of John W. Tukey (1984) Wadsworth, Inc., Belmont, CA.

M.J.R.H. on leave from Rothamsted Experimental Station, Harpenden, Herts.

Prepared in part in connection with research by J.W.T. at Princeton University sponsored by the Army Research Office (Durham).

Copyright © 1963 by John Wiley and Sons, Inc., New York, NY. Reprinted by permission, from (1963) *Proceedings of the Symposium on Time Series Analysis*. (Murray Rosenblatt, ed.) 209-243, John Wiley, New York.

naturally stated in frequency (or period) terms or could easily be converted into such terms. This chapter begins the study of the usefulness of spectrum techniques in problems naturally arising as, or easily convertible into, questions of the existence and timing of "echoes." It raised many more questions of importance to the analysis of data than it answers; we hope that others will become interested in these questions.

The need for such techniques arose in work on seismological data, where the arrivals of various waves or *phases* can be considered as the arrival of more or less distorted echoes. In the situation that concerned us the existence and timing of these echoes were not sufficiently apparent on the original seismograph traces or in the results of those direct manipulations of the original record that were tried. Accordingly, it was natural to ask if frequency methods could help. The present chapter outlines some of the resulting techniques, giving modest detail for those that seem most promising.

For general background on spectrum analysis, see [1] and [7]; for general background on seismology, see [3] and [4].

In general, we find ourselves operating on the frequency side in ways customary on the time side and vice versa. Experience has made it clear that "words that sound like other words," although strange at first sight, considerably reduce confusion on balance. These parallel or "paraphrased" words are made by the interchange of early consonants or consonant groups, as in "alanysis" from "analysis," and are introduced as needed. A complete list is given in Appendix 2.

In particular, we conclude that although the ordinary autocovariance or autocorrelation cannot be trusted to detect echoes, except in favorable circumstances, the more complex methods outlined here (involving the cepstrum or some form of pseudo-autocovariance) can be effective in a much larger variety of situations.

2. QUEFRENCY ALANYSIS AND THE CEPSTRUM

EFFECT ON THE POWER SPECTRUM OF A SIMPLE ECHO

In the simplest echo, values of a time series $y(t)$ are multiplied by a constant α (which may be negative), delayed by a time difference τ , and added to the original series to give a new series

For clarity
expressed
choice wou

The 1
original se
in sec⁻¹, so

whose log

ignoring t
series is t
which is
simply rel
log power
"frequenc
second o
considered
in the ap
frequency
ripple by
origin—the
described
terms we
ripple in
and saph

A ri
obscured
original s
the stretc
stretches
periodic
more or
obvious
autocova
we are l

$$z(t) = y(t) + \alpha \cdot y(t-\tau).$$

For clarity we shall write throughout as if τ and other times were expressed in seconds and all frequencies in sec^{-1} . Any other consistent choice would of course be equally correct.

The Fourier transform of the echo is obtained from that of the original series by multiplying by $\alpha \exp(2\pi i f \tau)$, where f is the frequency in sec^{-1} , so that if $\Phi(f)$ is the power spectrum of $y(t)$ then that of $z(t)$ is

$$\Phi(f)(1 + 2\alpha \cos 2\pi f \tau + \alpha^2)$$

whose logarithm is approximately

$$\log \Phi(f) + 2\alpha \cos 2\pi f \tau,$$

ignoring the terms in α^2 . The effect of adding the echo to the original series is thus relatively simple in terms of the log power spectrum, to which is added a (nearly) cosinusoidal ripple whose parameters are simply related to the echo parameters α and τ . Remembering that the log power spectrum is a function of the frequency f , it is clear that the "frequency" of the ripple is just τ , whose units are ripples per cycle per second or (necessarily) seconds. The log power spectrum can be considered as a "frequency series"; if estimated digitally (as it always is in the applications we shall describe here), it will in fact be a discrete frequency series. In such a series we describe a (nearly) cosinusoidal ripple by its *quefrency*, its *gamplitude*, and its *saphe* at some (frequency) origin—these are just the analogs of what in a time series would be described by frequency, magnitude (or amplitude), and phase. In these terms we can say that a simple echo of size α and delay τ produces a ripple in the log spectrum of quefrency τ , gamplitude approximately 2α and saphe (at zero frequency) 0 if α is positive and π if α is negative.

A ripple of this kind in the log spectrum will in practice be obscured to a greater or lesser degree by irregularities present in the original spectrum and by irregularities stemming from the finiteness of the stretch of data at hand—in the seismological application rather short stretches of data are of particular interest. The detection and study of periodic phenomena obscured by noise is a problem for which may more or less well-known techniques are available. Perhaps the most obvious consists in the procedures of spectrum estimation—autocovariance and Fourier transformation with a suitable window—and we are led to apply them to the frequency series provided by the log

spectrum of the original process. The result is appropriately termed the *cesptrum* or *cepstrum* of the original time series (by direct paraphrase, "spectrum" → "cesptrum," but ease of pronunciation seems doomed to lead to "cepstrum"). The cepstrum is a function of quefrency and is determined over a range extending from zero up to a maximum quefrency that is necessarily equal to the longest lag in the autocovariances used in the original power-spectrum calculations. A peak at a certain quefrency in the cepstrum suggests the existence of an echo with the corresponding delay in the original series.

THE CEPSTRUM OF SIMPLE ECHOES

An example of this technique applied to an artificial series with a simple echo with $\alpha = +0.5$ and $\tau = 5$ sec is shown in Figures 1 to 3. Figure 1 shows the autocovariance function (normalized and plotted as an autocorrelation function) out to a lag of 40 sec. Figure 2 is the log power spectrum, showing the ripple at a quefrency for 5 cycles/cps, and Figure 3 shows the cepstrum peaking at 5 sec.

The details of the preparation of this artificial series are rather closely related to the appropriate processing of real series and have noticeable importance. Starting with 470 random normal deviates, we "tapered" the first and last 10 percent and then added 185 zeros at each end. This tapering operation involves multiplication of the i th value from each end by $\frac{1}{2}[1 - \cos(\pi(i/47))]$, thus making a smooth transition from values multiplied by zero to those multiplied by unity. The resulting series was then multiplied by 0.5, delayed 50 terms, and added to itself. All our artificial series were constructed in this way, and they will be described as if there had been 10 observations/sec.

It will be apparent from Figure 1 that the echo shows up clearly where it might have been expected—as a peak in the autocovariance function at 5 sec lag. This, however, refers to an ideal case in which the original spectrum is smooth (in fact white) and the echo an exact scaled copy of the original. Figures 4 to 7 refer to an example in which the original spectrum is somewhat more complex. The 5-sec peak is still present in the autocovariance (Figure 4), but it is noticeably less clearly defined. The log spectrum is shown in Figure 5 and clearly shows the expected ripple, but, from our present viewpoint, its most obvious feature is the low quefrency arch corresponding to the (green, by analogy) spectrum of the original unechoed series. Before estimating the spectrum of such a series in the time domain, we would naturally think of prewhitening with a suitable high-pass filter, and in the same way we can apply a *long-pass lifter*. We have used a Chebyshev type of lifter with 21 terms whose power transmission is zero at zero quefrency and

varies between 0.9 and 1.0 in the pass band. The result is a liftered log spectrum.

Figure 7—comparison of the original and liftered spectra.

This artificial series has a "green" spectrum characterized by a low-frequency peak, echoing, and comb filtering. The effect of linear time-shift-invariant filtering (here $y_i - 0.98y_{i-2}$) to the spectrum is shown in Figure 8. The filtering was in fact done.

Figures 8 and 9 show the effect of filtering on the spectrum of an irregular bandpass noise sample. The spectrum of the original (Figure 9) is now compared with the spectrum (Figure 10) and the cepstrum (Figure 11) of the ideal spectrum (Figure 12).

Used in conjunction with the spectrum (poor choice of filter), the cepstrum is effective in revealing the presence of an echo. The autocovariance fails to do this.

COMPLEX ECHOES

Our simple echo example can be generalized in various ways. (1) From the "direct signal" case to the case of transmitted or (2) reflected signals at different frequency.

If the strength of the echo is small enough, the ripple in the spectrum will be small. Suppose we represent the spectrum of the original signal and the spectrum of the echo by the Fourier transforms

Then the power spectrum of the sum is

$$S(f) = S_1(f) + S_2(f) + 2\int_{-\infty}^{\infty} S_1(f') S_2(f-f') df'$$

varies between 0.9927 and 1.0073 for quefrequencies above 2 sec. The liftered log spectrum is shown in Figure 6 and the cepstrum in Figure 7—comparison of Figure 7 with Figure 3 reveals only minor changes.

This artificial series could have been made by first imposing the "green" spectrum on the original series by filtering and then tapering, echoing, and combining. Since filtering and echoing (which are both linear time-shift-invariant operations) commute, it was easier to apply the filtering (here with coefficients (1.00, 0.00, -0.98), taking y_i into $y_i - 0.98y_{i-2}$) to the tapered and echoed series of the first example, as was in fact done.

Figures 8 and 12 relate to a more extreme example, which is closer to the realities of the seismological problem. The same (white-noise plus echo) series has now been prefiltered by a narrow and rather irregular bandpass filter whose effect on the log spectrum of a white-noise sample is shown in Figure 8. The spike in the autocovariance (Figure 9) is now almost wholly masked, but the ripple in the log spectrum (Figure 10) is still quite clear. Liftering produces Figure 11, and the cepstrum (Figure 12) is again little changed from that for the ideal spectrum (Figure 3).

Used in conjunction with judicious liftering of the log power spectrum (poor choices of lifter have given us noticeable difficulty), the cepstrum is effective in detecting simple echoes when the autocovariance fails completely.

COMPLEX ECHOES AND RAHMONICS

Our simple echo, characterized by one fixed α and one τ , can be generalized in various ways. If the "echo" travels by a different path from the "direct signal," there is no reason for (1) the relative intensities transmitted or (2) the relative time delays to be independent of frequency.

If the strength of the echo is frequency-dependent, the height of the ripple in the log power spectrum will depend on frequency. Suppose we represent the sum of the original series and its distorted echo by the Fourier transform of

$$F(\omega) + G(\omega)e^{i\omega\tau}.$$

Then the power spectrum of the combined series is given by the squared modulus of this expression,

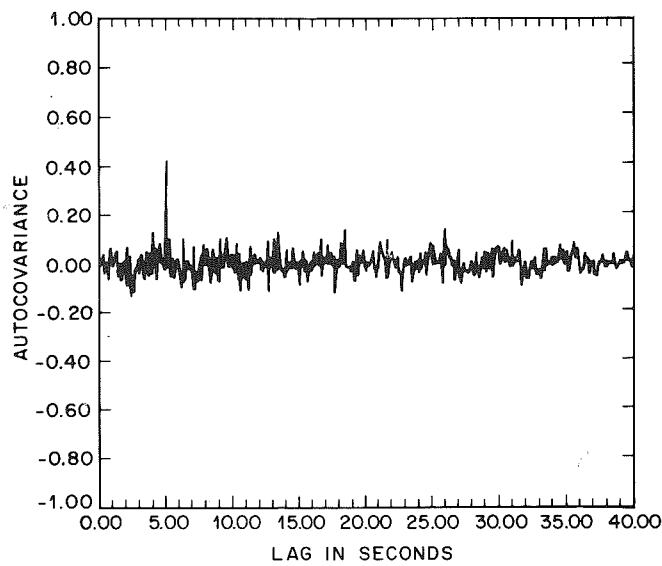


Figure 1. Normalized autocovariance of an artificial series of white noise with a simple echo of amplitude -0.5 and delay 5.0 sec.

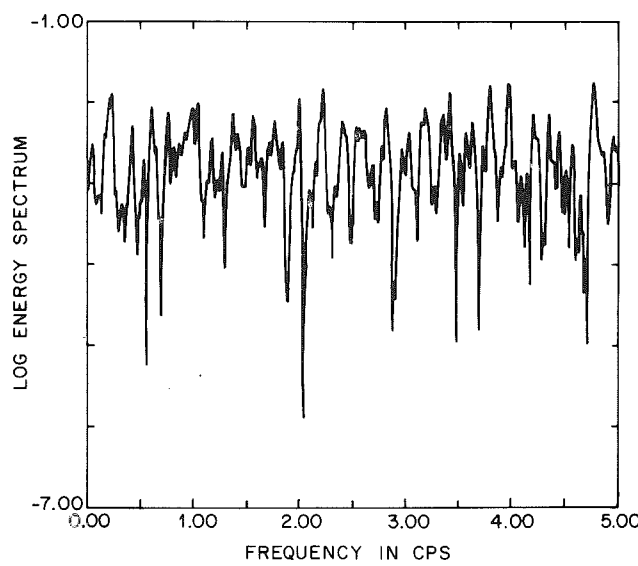


Figure 2. Log energy spectrum of an artificial series of white noise with a simple echo of amplitude -0.5 and delay 5.0 sec.

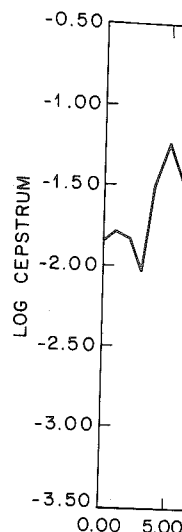


Figure 3. Log cepstrum of an artificial series of white noise with a simple echo of amplitude -0.5 and delay 5.0 sec.

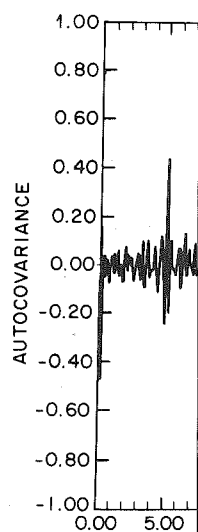


Figure 4. Normalized autocovariance of an artificial series of white noise ("green" echo) with a simple echo of amplitude -0.5 and delay 5.0 sec.

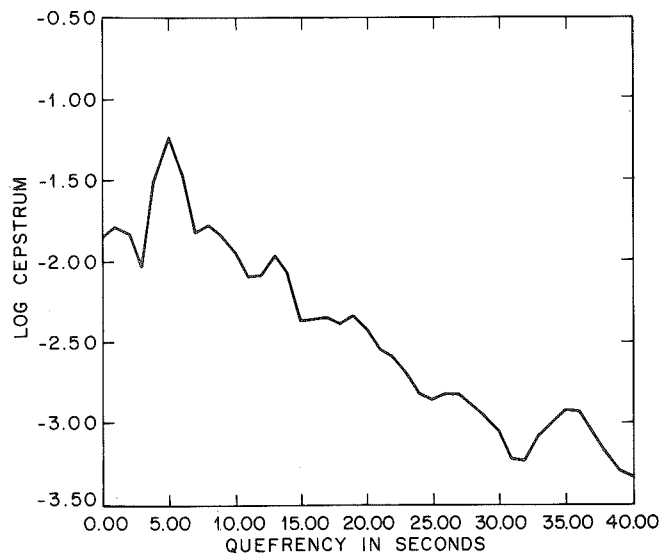


Figure 3. Log cepstrum of an artificial series of white noise with a simple echo of amplitude -0.5 and delay 5.0 sec.

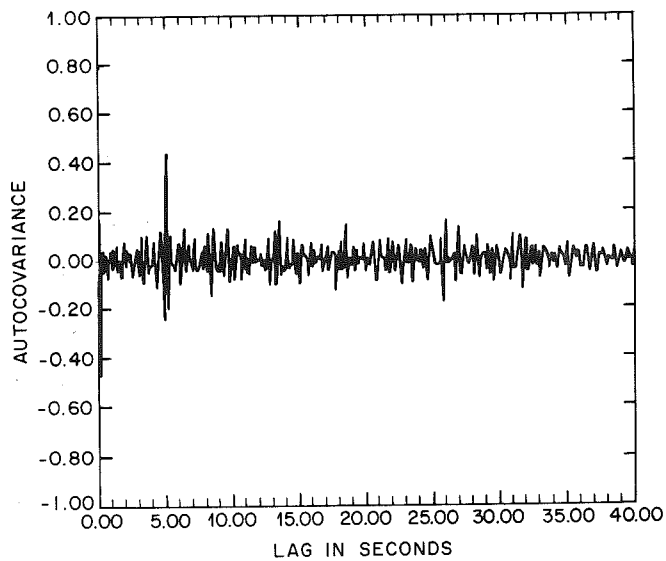


Figure 4. Normalized autocovariance of an artificial series of "green" noise ("green" filter coefficients $1.0, 0.0, -0.98$) with a "green" echo of amplitude -0.5 and delay 5.0 sec.

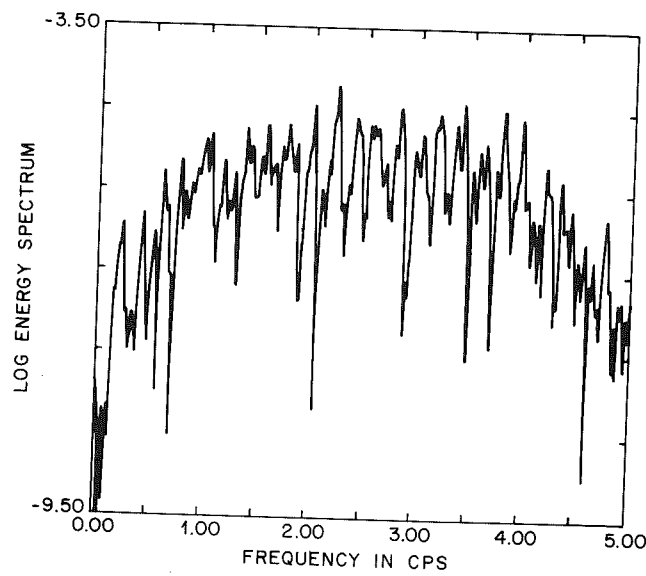


Figure 5. Log cepstrum of "green" noise plus "green" echo.

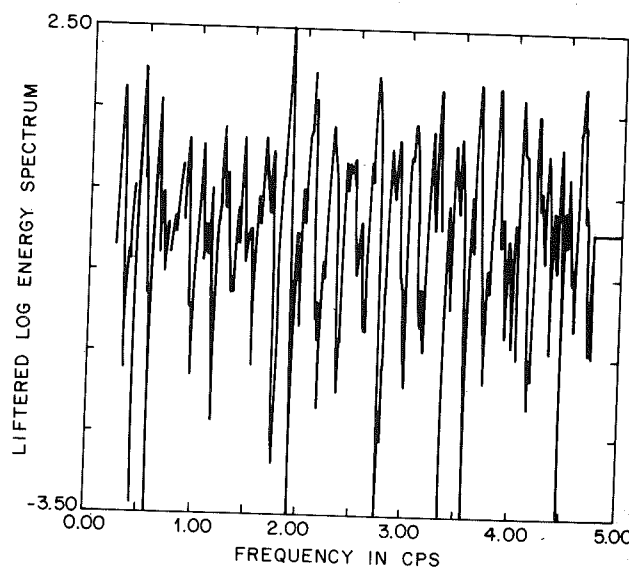


Figure 6. Liftered log energy spectrum of "green" noise plus "green" echo. Lifter is Cebyshev type 21 coefficient long pass with frequency cutoff at 2 sec.

Figure

Figure 8.

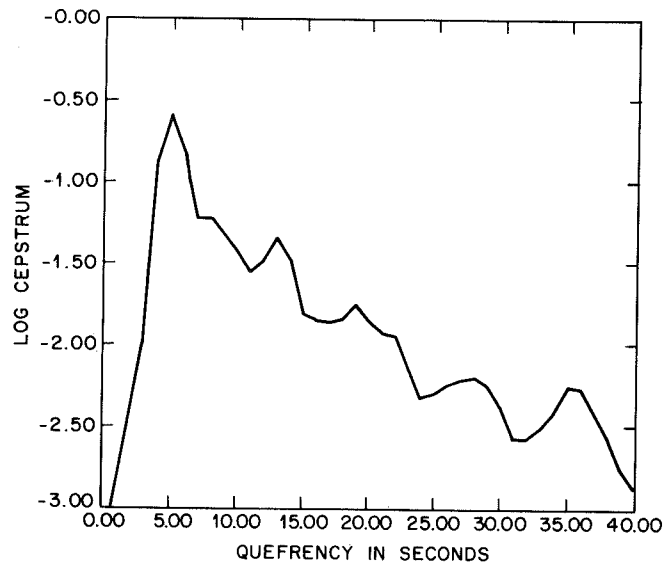


Figure 7. Log energy spectrum of "green" noise plus "green" echo.

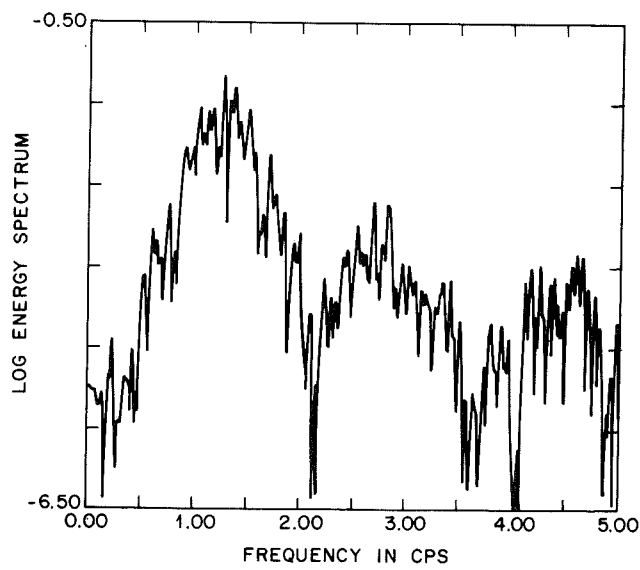


Figure 8. Log energy spectrum of a stretch of white noise filtered by a 41-coefficient irregular bandpass filter to indicate its transmission.

"green"
ass with

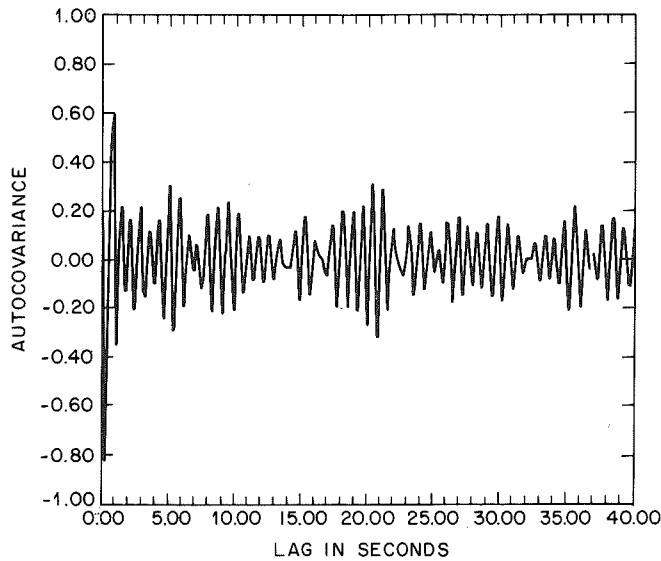


Figure 9. Normalized autocovariance of filtered white noise plus filtered white echo.

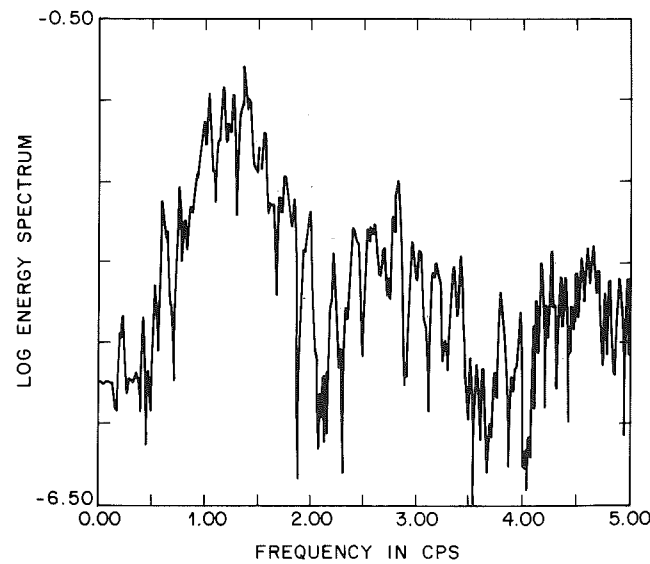


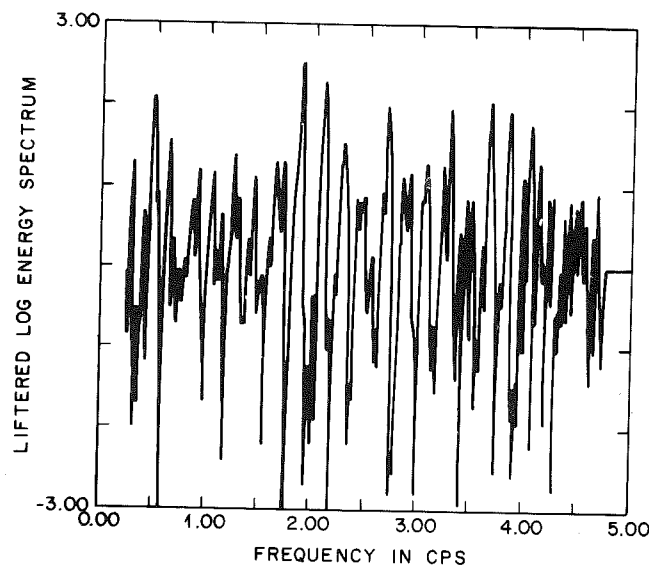
Figure 10. Log energy spectrum of filtered white noise plus filtered white echo.

Figure 11

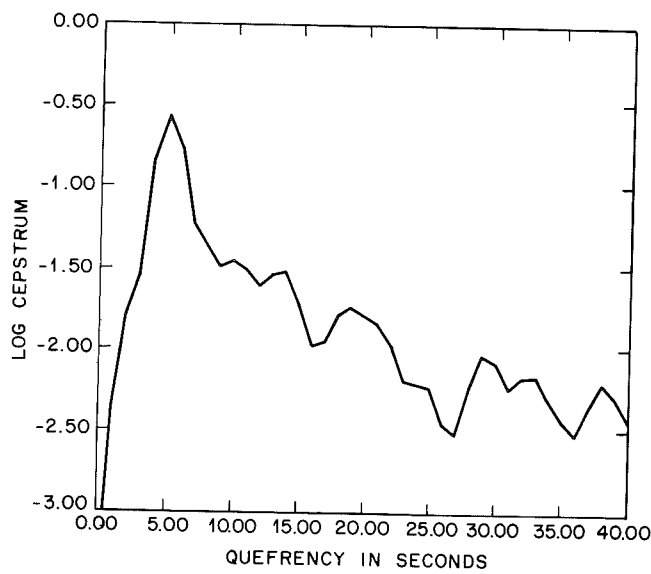
LOG CEPSTRUM

Figure 12.

12. THE QUEFRENCY ALANYSIS OF TIME SERIES FOR ECHOES 465



plus
Figure 11. Liftered log energy spectrum of filtered white noise plus filtered white echo.



tered
Figure 12. Log cepstrum of filtered white noise plus filtered white echo.

$$|F|^2 + |G|^2 + 2|F||G|\cos(\omega\tau + \theta(\omega)),$$

where $\theta(\omega) = \arg F(\omega) - \arg G(\omega)$. Thus the gamnitude of the ripple in the log spectrum is approximately

$$2|F||G|/(|F|^2 + |G|^2) = \operatorname{sech}(\log|F| - \log|G|).$$

Changes in time delay with frequency will cause the quefrency of the ripple to change as the frequency changes. If this change is sufficiently small, the varied quefrequencies will all contribute to a single cepstrum estimate and no difficulty will arise. If, on the other hand, the change spreads the ripple's quefrequencies over what would ordinarily be many cepstrum estimates, special methods of analysis, effective only when closely adapted to a known pattern of delay, would be required. Fortunately, this situation is not to be expected in the application to seismic body waves, though it might complicate a similar study of surface waves.

The effects of the nonlinear terms in the power series for $\log(1+x)$ deserve some attention. In the case of a single α and τ

$$\begin{aligned} \log(1 + 2\alpha \cos 2\pi f \tau + \alpha^2) \\ &= (2\alpha \cos 2\pi f \tau + \alpha^2) - \frac{1}{2}(2\alpha \cos 2\pi f \tau + \alpha^2)^2 + \dots \\ &= \alpha^2 + 2\alpha \cos 2\pi f \tau - 2\alpha^2 \cos^2 2\pi f \tau + \dots \end{aligned}$$

but

$$2\alpha^2 \cos^2 2\pi f \tau = \alpha^2 + \cos 4\pi f \tau,$$

so that the final result to quadratic accuracy is

$$2\alpha \cos 2\pi f \tau - \alpha^2 \cos 4\pi f \tau.$$

The second *rahmonic* (cp. harmonic) represented by the term $\alpha^2 \cos 4\pi f \tau$ contributes an amount $\frac{1}{2}(\alpha^2)^2$ to the variance of the ripple. This is to be compared with the contribution $\frac{1}{2}(2\alpha)^2$ of the fundamental. The ratio is $\alpha^2/4$, so that rahmonics, although to be expected, should be rather small.

Another
would be pr
 α_2, τ_2 . These

and the pow

$1 + 2\alpha_1 \cos$

so that the a

$2\alpha_1 \cos 2$

to quadratic
we expect a
twice that of
to this order
replaced the
spectrum by
(When high
remains.)

Although
obviously b
spectroscopy ha

THE CE

Figures
spectrum di
produced by
surrounded
with coeffici
coefficients (br
added to the
bandpass filt
the autocova

Another source of complexity, which is to be expected in practice, would be provided by multiple echoes with parameters (say) α_1, τ_1 and α_2, τ_2 . These would multiply the original Fourier transform by

$$1 + \alpha_1 e^{2\pi i f \tau_1} = \alpha_2 e^{2\pi i f \tau_2},$$

and the power spectrum by

$$1 + 2\alpha_1 \cos 2\pi f \tau_2 + 2\alpha_2 \cos 2\pi f \tau_2 + 2\alpha_1 \alpha_2 \cos 2\pi f (\tau_1 - \tau_2) + \alpha_1^2 + \alpha_2^2,$$

so that the amount added to the log spectrum is

$$\begin{aligned} & 2\alpha_1 \cos 2\pi f \tau_1 + 2\alpha_1 + 2\alpha_2 \cos 2\pi f \tau_2 - \alpha_1^2 \cos 4\pi f \tau_1 - \alpha_2^2 \cos 4\pi f \tau_2 \\ & - 2\alpha_1 \alpha_2 \cos 2\pi f (\tau_1 + \tau_2) \end{aligned}$$

to quadratic accuracy. Thus, in addition to ripples at quefrequencies τ_1, τ_2 , we expect a ripple at quefrecency $(\tau_1 + \tau_2)$ with gamnitude of the order of twice that of the rahmonics at quefrequencies $2\tau_1, 2\tau_2$. It is of interest that, to this order of approximation, the logarithmic transformation has replaced the difference ripple at quefrecency $(\tau_1 - \tau_2)$ present in the spectrum by one of equal gamnitude at the sum quefrecency $(\tau_1 + \tau_2)$. (When higher orders of approximation are used, the difference ripple remains.)

Although sorting out even a moderate number of echoes will obviously become difficult (a comparable problem is familiar in spectroscopy), echo complexity in general seems likely to be quite effectively handled by the cepstrum.

THE CEPSTRUM OF COMPLEX ECHOES: EXAMPLES

Figures 13 to 16 relate to an artificial series in which the echo spectrum differs markedly from that of the original. This series was produced by taking a set of random normal deviates, tapered and surrounded by zeros, and producing first a "pink" series by filtering with coefficients (1.00, 0.98) and then a "blue" series by filtering with coefficients (1.00, -0.98). The second series was delayed 50 terms and added to the first, and the result was then passed through the irregular bandpass filter previously referred to. The echo is quite undetectable in the autocovariance (Figure 13), but the ripple shows up in the liftered

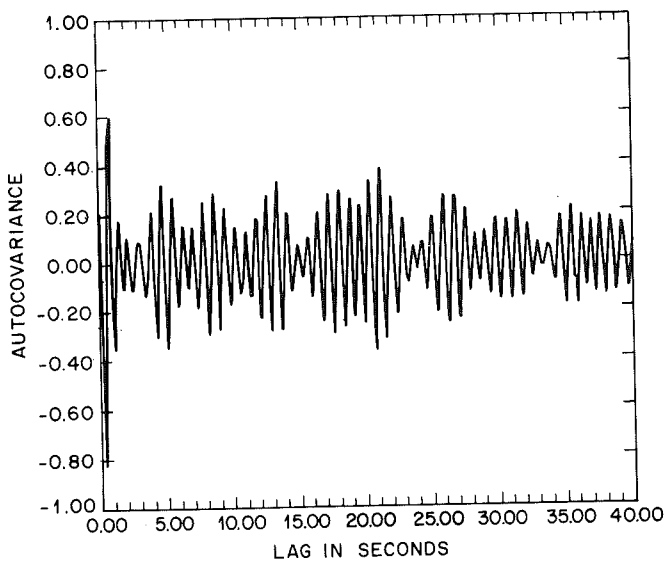


Figure 13. Normalized autocovariances of filtered "pink" noise plus filtered "blue" echo. "Pink" filter coefficients 1.0, -0.98. "Blue" filter coefficients 1.0, 0.98.

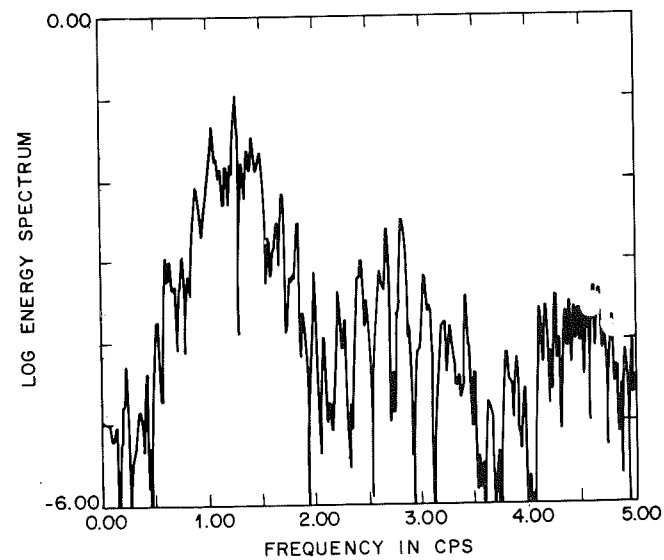


Figure 14. Log energy spectrum of filtered "pink" noise plus filtered "blue" echo.

LIFTED LOG ENERGY SPECTRUM

2.50
-3.50
0.00

Figure 15. Lifted log energy spectrum of filtered "pink" noise plus filtered "blue" echo.

LOG CEPSTRUM

0.00
-0.50
-1.00
-1.50
-2.00
-2.50
-3.00
0.00

Figure 16. Log cepstrum of filtered "pink" noise plus filtered "blue" echo.

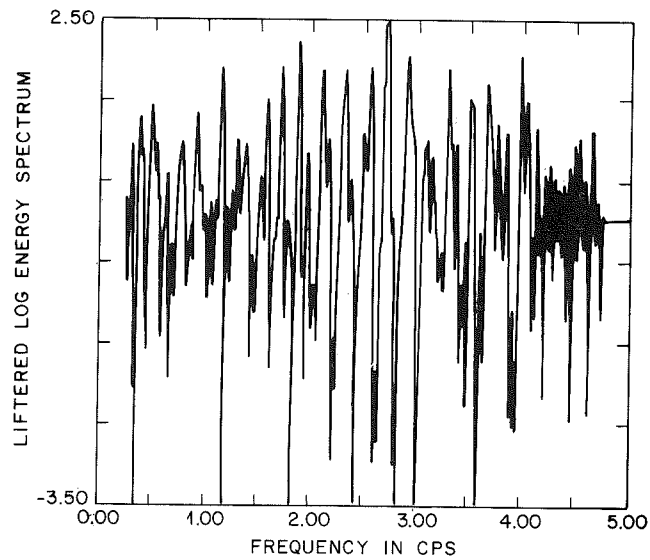


Figure 15. Liftered Log energy spectrum of filtered "pink" noise plus filtered "blue" echo.

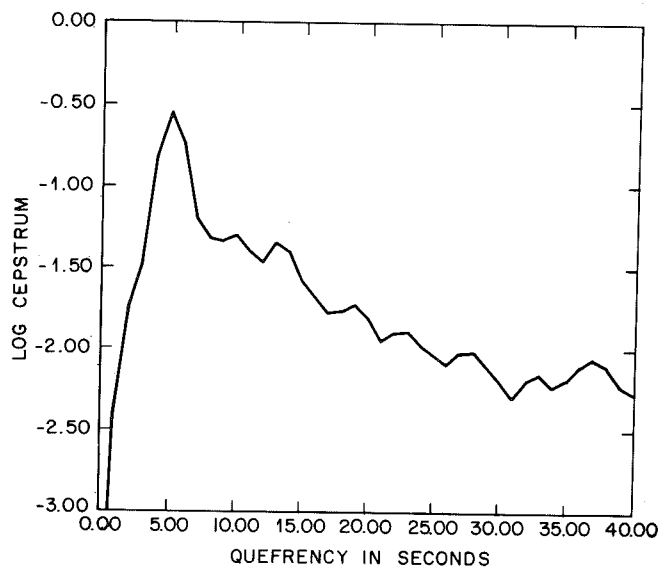


Figure 16. Log cepstrum of filtered "pink" noise plus filtered "blue" echo.

log spectrum with its gamnitude varying across the frequency band in the way expected, and a clear peak is evident in the cepstrum (Figure 16).

COMPARISON WITH AUTOCORRELATION

We have given evidence that autocorrelation is more likely to fail to detect complex echo than are the more elaborate processes we have been developing. It is important to understand why this is so. It is natural to think of the dualism between time and frequency as an either-or phenomenon—sometimes we look at things one way, sometimes the other. Insofar as actual time series are concerned, the situation is often far more *both* than either. Series containing echoes, whether or not geophysical, are not likely to have had a white spectrum before the echo was added in. Some may have had a spectrum that was smooth enough to give the autocorrelation a fighting chance to find the echo, but many have not.

We could always try to proceed by first finding the power spectrum of the original series and then calculating a filter that, when applied to the original series, would approximately smooth out the short-quefrency variations in the spectrum. Then we could apply this filter to the original data and calculate the autocorrelation of the resulting series. On the other hand, we could try many alternative filterings of the original series and then look at the autocorrelation of that one whose spectrum was relatively free of short-quefrency components (i.e., trends with frequency). Such procedures would surely be no easier than these we suggest. Their only advantage would seem to be that they would allow one to whom the autocorrelation is sacred to apply it.

The usefulness of the more nonlinear processes lies in the fact that liftering the log power spectrum removes the effects of short-quefrency components without any need for recognizing their individuality.

3. PSEUDO-AUTOCOVARIANCES

RATIONALE AND EXAMPLES

One key operation in the use of the cepstrum seems to be the liftering of the log (estimated) power spectrum. To produce the cepstrum, this has to be followed by a further quadratic transformation. Since finding the log (estimated) power spectrum already involves taking the logarithm of results from a quadratic transformation, it is natural to ask if all this piling of nonlinearity on nonlinearity is necessary. Can we omit the nonlinearity of the last step?

A natural move back to the liftered lo [which make could approp of lag or delay We have cho value equal to

We must autocovariance it might not b a function of reasonable. W

Figures the delogged autocorrelation case there wa comparison of original spectrums autocorrelation pseudo-autocor liftering the success of the

IS IT BETTER?

Although prominent in corresponding conclusions about further nonlinearities calculate, not changes of τ were to obtain a pseudo-autocorrelation.

Moreover, will show the ordinary autocorrelation sampling fluctuations expected to shift estimates.

* In some later autocovariance —

A natural suggestion is to take the liftered log power spectrum and move back toward the autocovariance. The Fourier transform of either the liftered log (estimated) power spectrum itself or of its antilogarithms [which make up the delogged liftered log (estimated) power spectrum] could appropriately be called a *pseudo-autocovariance**. Such a function of lag or delay will not automatically be normalized in any natural way. We have chosen to scale the result by making its maximum absolute value equal to unity.

We must emphasize that this whole inquiry into pseudo-autocovariances is quite thoroughly empirical. We do not know, though it might not be hard to establish, whether it is reasonable to regard such a function of the original data as estimating something definite and reasonable. We are exploring with only heuristic guidance.

Figures 17 to 20 show the pseudo-autocovariances obtained from the delogged liftered log power spectra corresponding to the autocorrelations of Figures 1, 4, 9, and 13, respectively. In the first ideal case there was nothing to gain from the involved process, but the comparison of Figures 9 and 19 is quite a different matter. When the original spectrum is complex enough to conceal the echo in the autocorrelation, the echo appears clearly and unmistakably in the pseudo-autocovariance. This fact provides support for our belief that liftering the log power spectrum was one of the vital steps in the success of the cepstrum.

IS IT BETTER THAN THE CEPSTRUM?

Although the peaks in our pseudo-autocovariances are at least as prominent in relation to their background as are those in the corresponding cepstra, we must pause before jumping to any conclusions about relative merit. The pseudo-autocovariance avoids a further nonlinear operation, but it requires more multiplications to calculate, not fewer. And it is, for example, not at all immune to small changes of τ with frequency. Although we understand rather well how to obtain a relatively satisfactory cepstrum, our understanding of pseudo-autocovariance is comparatively quite small.

Moreover, it is natural to anticipate that pseudo-autocovariances will show the complexly interrelated sampling fluctuations for which ordinary autocorrections and autocovariances are well known. The sampling fluctuations of cepstrum estimates, on the other hand, can be expected to show the simple and desirable behavior typical of spectrum estimates.

* In some later papers, the term *pseudo-autocorrelation* is used in place of pseudo-autocovariance — Ed.

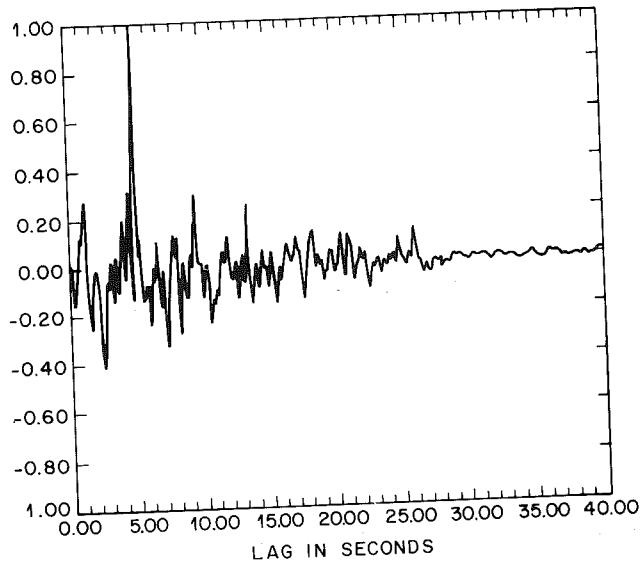


Figure 17. Pseudo-autocovariance of white noise plus white echo.
Liftered log spectrum was delogged.

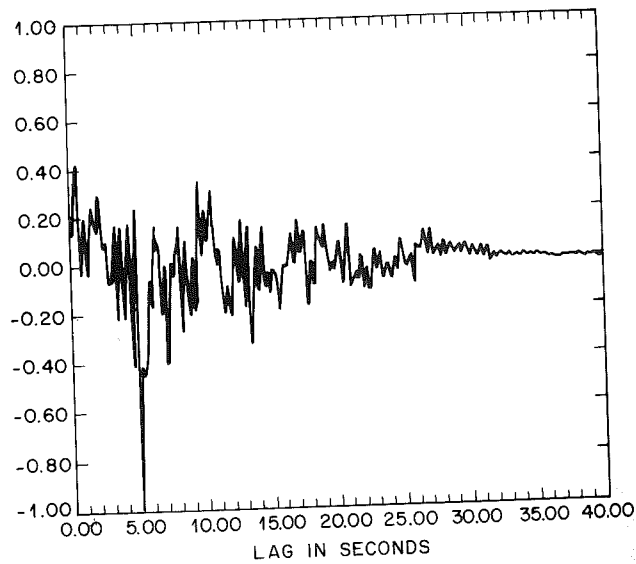


Figure 18. Pseudo-autocovariance of "green" noise plus "green" echo.

Figure 19. P
"T

Figure 20. P
"V

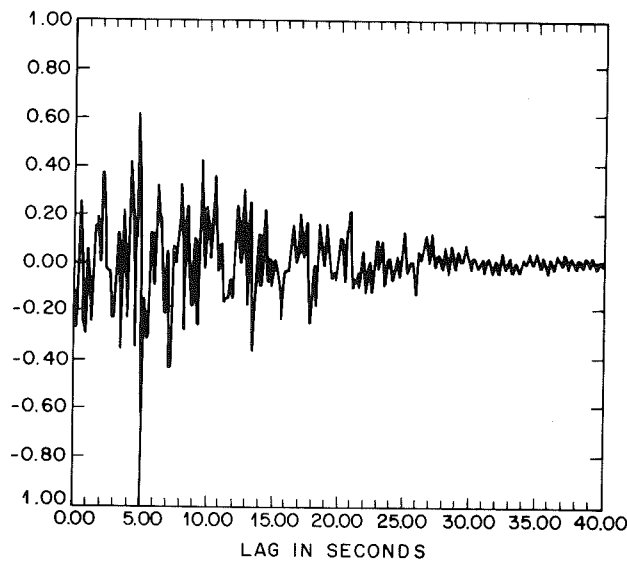


Figure 19. Pseudo-autocovariance of filtered "pink" noise plus filtered "blue" echo.

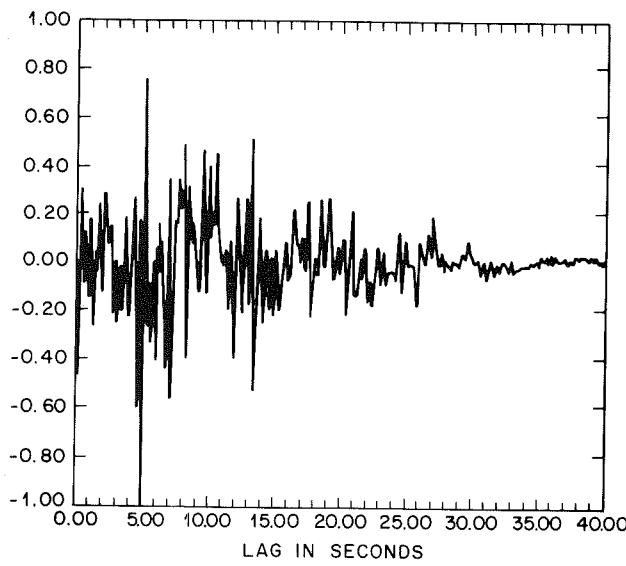


Figure 20. Pseudo-autocovariance of filtered white noise plus filtered white echo.

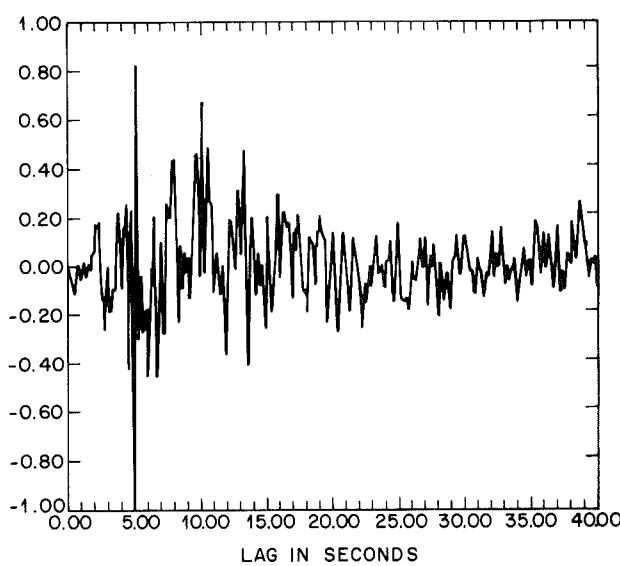


Figure 21. Pseudo-autocovariance of filtered "pink" noise plus filtered "blue" echo. The filtered log spectrum was not delogged.

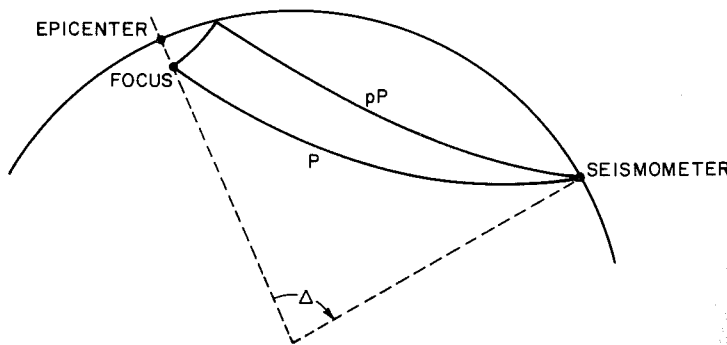


Figure 22. Seismic body wave paths of interest in focal depth determination at large epicentral distances Δ .

It will take substantial experience and exploration before we can choose wisely between cepstrum and pseudo-autocovariance.

ALTERNATIVE FORMS

Figure 21 shows the result of transforming back the liftered log power spectrum itself, omitting the delogging operation. Comparison with Figure 20 shows few detailed resemblances, apart from the noticeable echo. The one seems smoother at short lags, the other at long ones; reasons for this are obscure to us.

As of the moment, we have in fact almost no insight into why one detailed calculation of a pseudo-autocovariance would be preferred to another. With further experience it may be possible to make improvements in this approach. Explorations into the effects of liftering the spectrum itself rather than its logarithmic form before Fourier retransformation (which would be an over-all quadratic process) or of retransforming the log of the unliftered power spectrum are two examples.

All that can be said now is that pseudo-autocovariances are promising but not understood.

is filtered
logged.

TER

al depth

4. THE SEISMIC PROBLEM

GEOPHYSICAL BACKGROUND

Our interest in the problem of echo determination arose from a desire to know the depth of a seismic disturbance. Knowing the depth would be helpful in differentiating between man-made and natural seismic events, as the modal depth of earthquakes is about 25 km and it is very unlikely that a seismic signal originating from depths greater than, say, 10 to 15 km would be man-made.

Most natural earthquakes result from the rapid release of stress which has built up slowly over periods measured in years. The stress release occurs when the rock gives way in shear, and part of the stored energy is released in elastic waves. The initial phases of the waves leaving in various directions differ by 0 or π . Man-made earthquakes are produced by explosions of one kind or another.

The location of the seismic source is called the *hypocenter*, its distance below the earth's surface is the *focal depth*, and the position on the surface directly above the source is the *epicenter*. The *epicentral*

distance is the great circle distance between the epicenter and the receiving seismometer.

Seismic waves travel through the earth (body waves) or along the earth's surface (surface waves). Body waves are two types—compressional or *P*-waves and shear or *S*-waves. *P*-waves travel with higher velocity than *S*-waves and both propagate along ray paths that are concave upward. Some may, in fact, be reflected from the surface several times before reaching the receiving seismometer. Each group of waves with a (possibly) distinct arrival is called a *phase*. The particular phases of interest to us are visible for epicentral distances greater than 25 to 30 degrees, and are shown on Figure 22. The phase taking the direct path is labeled *P*, and the other path includes a reflection from the surface near the source. If the wave traveling from the source to the surface is a *P*-wave, the phase is called *pP*. If the wave from source to surface is an *S*-wave, the phase is called *sP*. The time interval between the arrival of *P* and *pP* or *sP* is almost directly proportional to the focal depth, with a small dependence on the epicentral distance from the receiver. The waves arriving at a receiver have the sequence *P*, *pP*, *sP*, followed usually after a longer time interval by other phases. If the focal depth is great enough, the *pP*- or *sP*-phases are delayed sufficiently that they can be observed as definite arrivals distinguished from the reverberation accompanying the *P*-phase. If the earthquake is shallow (less than about 60 km focal depth), the *pP*- and *sP*-phases are obscured by the reverberation and we are forced to use other methods to find these echoes.

The transmission of seismic body waves is complicated by reflection at irregularities in the medium, both near the source and near the receiver so that a simple source pulse will be spread out in time by reverberation. During transmission the frequency content will change as higher frequencies (e.g., 10 to 100 cps) are absorbed so that at large distances the highest frequencies observed are about 2 to 4 cps. Dispersion of body waves (dependence of velocity on frequency) is small enough to be ignored.

Surface waves owe their existence to the free surface of the earth and are of two types: Love waves and Rayleigh waves. Love waves are analogous to *S*-waves and may be regarded as horizontally polarized shear waves guided by the earth's surface. Rayleigh waves have a vertical component of particle motion and are similar to surface water waves (except that the elliptical particle motion is retrograde). For Rayleigh waves to exist, there must be both a free surface and a variation of velocity with depth in the medium. Because of this velocity gradient, surface waves show considerable dispersions. We have not tried to apply analysis techniques to surface waves, although they may be useful in the study of multipath surface-wave propagation.

There are three methods in use. Method one, explained for large epicentral distances, gives the arrival times of the *P*-wave at receiving stations from which the epicenter can be located. This method is useful for earthquakes in the central and eastern parts of the USSR where a network has been established. The USSR network, which covers the entire country, gives an accurate determination of epicentral distance. Method one cannot be used for large epicentral distances because it does not give an accurate arrival time. Method two [5], which resembles method one, gives an accurate determination of certain phases observed on the seismograms discussed here. In summary, method one is the best and, except for nearby events, gives an accurate determination of epicentral distance.

Figure 23 shows some short-period Benioff seismic waves. The accurate determination of the epicentral distance is not a simple matter. The first phase, which probably corresponds to the *pP* phase, can be read as *pP* and the second phase, which corresponds to the *sP* phase, can be read as *sP*. The time interval between the two phases is the same as the time interval between the two peaks in the spectrum, but the arrival times cannot easily be determined.

SEISMIC APPLICATIONS

In attacking the geophysical problems of seismic wave propagation analysis has to compete with the work of seismologists and geophysicists who study long wave trains without regard to the source. The situation is almost at the opposite extreme. The seismic waves are limited in duration (giving rise to a sharp peak in the spectrum) and have relatively abrupt start and end points.

The problem that has been described here thus provides a good opportunity for the application of cepstrum analysis to seismic waves. Accordingly, we have applied cepstrum analysis to the original problem of determining the epicentral distance and have obtained a solution to an important problem which is not yet fully understood.

The cepstrum and power spectrum of the seismic waves shown in Figure 23 are shown in Figure 24. The spectrum has no features as defined by equation (1). Certain peaks appear in the spectrum, but they are not autocovariances of a periodic function.

There are three methods of focal depth determination currently in use. Method one, explained above, is useful for deep earthquakes at large epicentral distances. Method two utilizes precise determination of arrival times of the P -waves at a dense network of nearby seismic receiving stations from which slant range is determined. This method is useful for earthquakes in California, Japan, New Zealand, and in certain parts of the USSR where seismic networks of sufficient density have been established. The U. S. Coast and Geodetic Survey in its computer determination of epicentral locations from arrival times recorded worldwide, gives an approximate focal depth using slant range if method one cannot be used. This method is not considered accurate for large epicentral distances. Method three, proposed by H. I. S. Thirlaway [5], resembles method one, but involves the relative times of arrival of certain phases observed only at nearby stations which have not been discussed here. In summary, accurate depth determination is difficult and, except for nearby events or deep distant ones, almost impossible.

Figure 23 shows some typical seismograms recorded on a vertical short-period Benioff seismometer at Chester, N.J. It is clear that the accurate determination of the arrival time even of the initial P -phase is not a simple matter. There are indications on the records that would probably be read as pP and sP by a trained seismologist, but again the arrival times cannot easily be fixed except within rather wide limits.

SEISMIC APPLICATIONS

In attacking the geophysical depth of focus problem, time series analysis has to compete with "eyeball" methods as applied by skilled seismologists and geophysicists. Analysis would be most favored by long wave trains without clear beginnings or endings. The actual situation is almost at the opposite pole: the wave trains are quite limited in duration (giving less chance for computational averaging) and have relatively abrupt starts (favoring visual recognition).

The problem that led to the techniques of time series analysis described here thus provides one of the situations least favorable to their use. Accordingly, we feel that successful application in the original problem is not to be unequivocally expected, either as a solution to an important problem or as a sign that the technique is useful.

The cepstra and pseudo-autocovariances of the earthquakes of Figure 23 are shown in Figures 24 to 29. It is at once evident that these have no features as definite as those shown by our artificial series. Certain peaks appearing both in the cepstrum and the pseudo-autocovariances of a particular series may be associated with the pP - and

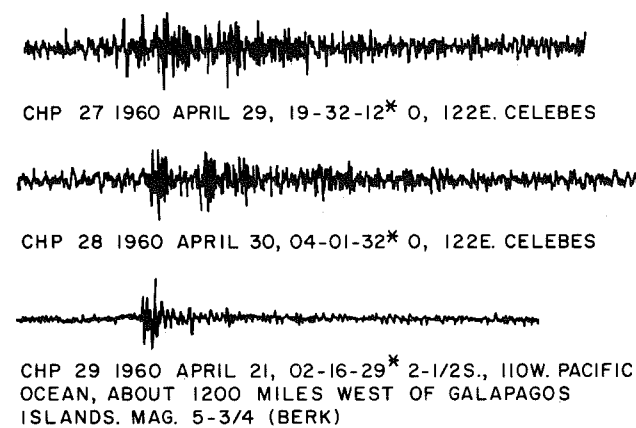


Figure 23. Seismograms of the earthquake records used in analysis.
(Photo B62-6733-MH.)

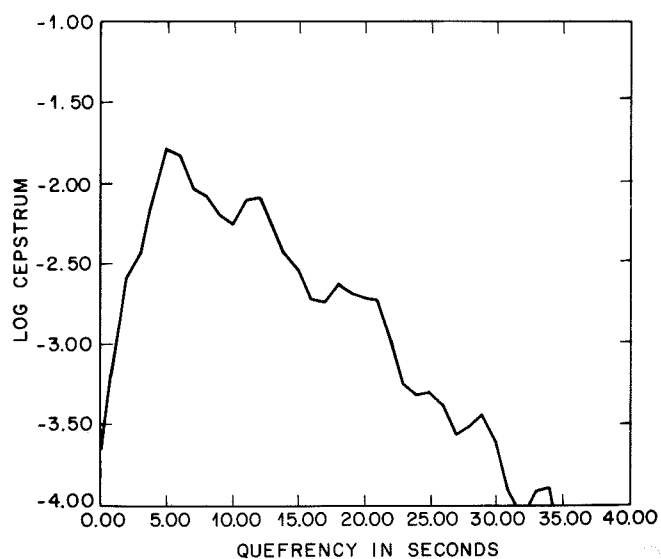


Figure 24. Log cepstrum of CHP27.

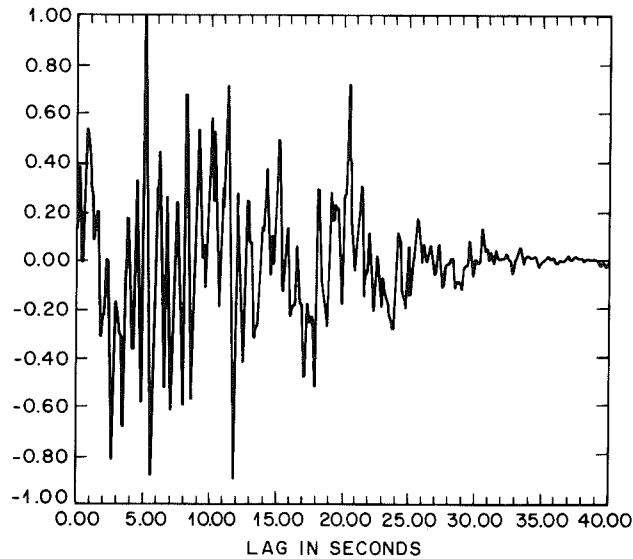


Figure 25. Pseudo-autocovariance of CHP27.

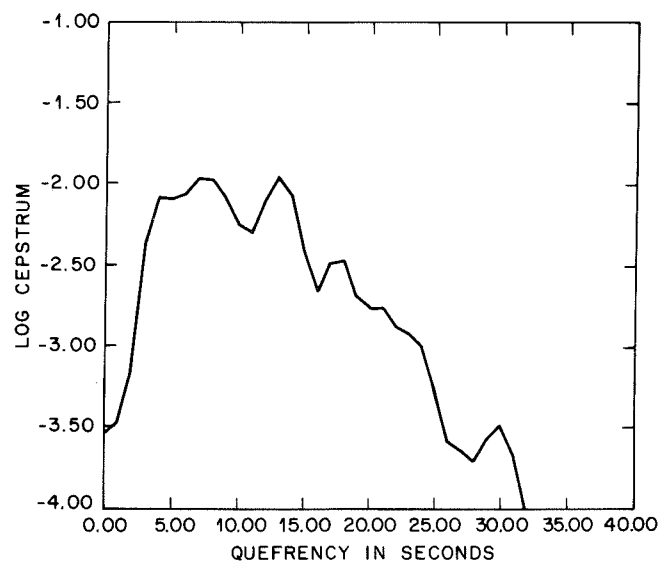


Figure 26. Log cepstrum of CHP28.

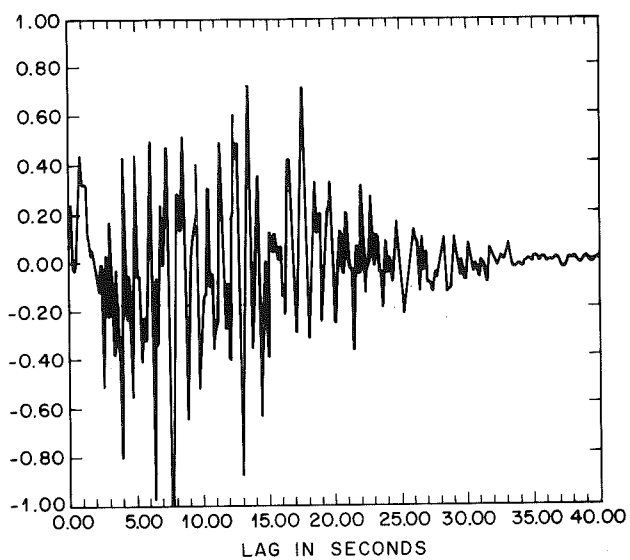


Figure 27. Pseudo-autocovariance of CHP28.

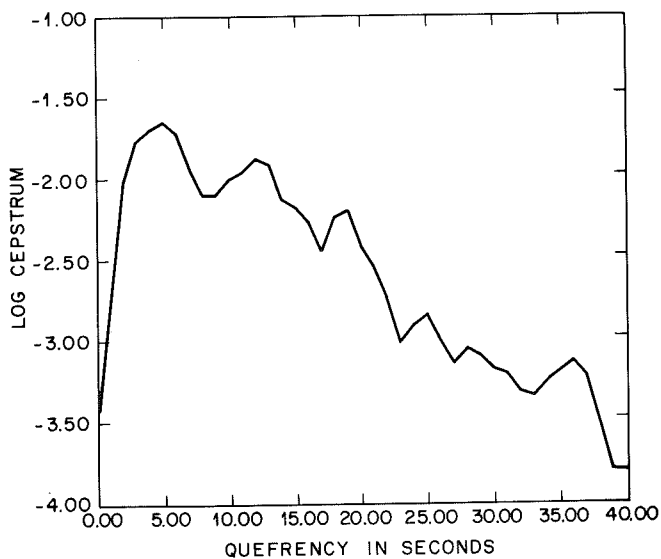


Figure 28. Log cepstrum of CHP29.

Figure

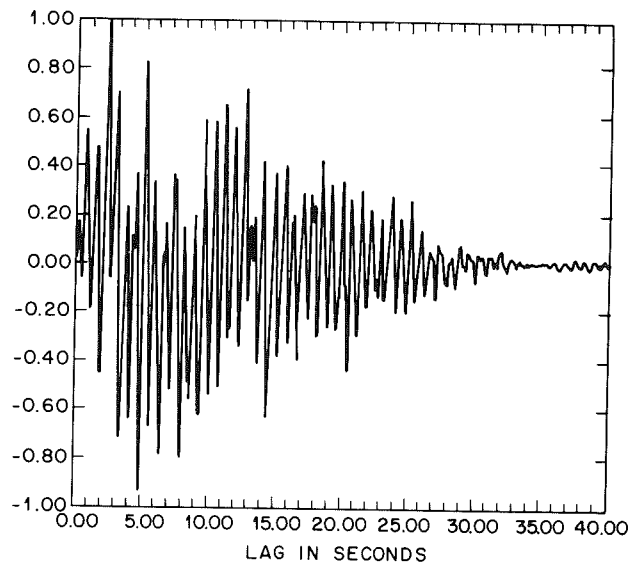


Figure 29. Pseudo-autocovariance of CHP29.

sP-phases. Until we know more about the properties of our new techniques, we do not feel that detailed discussion of these records would be profitable.

The cross c

(cocepstrum) +

5. CROSS-CEPSTRUM ALANYSIS

THE TWO-RECEIVER PROBLEM

Echoes of body waves from earthquakes can be expected to occur both near the source and near the receiver (seismometer). In the present problem we recognize only the echoes near the source, rejecting those near the receiver. This is clearly impossible so long as we are analyzing (specifically alanyzing) records from a single receiver.

If we have records of the same event made at two widely separated stations, however, source-end echoes may be identified by their occurrence in both records, whereas receiver-end echoes occur in only one. What is needed is a quefrency alanyzis that will detect matched ripples in the two records. As Mr. Gordon Newstead of the University of Tasmania suggested to us, the *cross cepstrum* of the two records (the result of applying cross-spectrum analysis to the two liftered log power spectra) has exactly the desired property, since only ripples from source-end echoes will be present in *both* liftered log power spectra.

For the present p

For a first a
appropriate to c
Another choice
(with quefrenc
and π (since th
following up th
fluctuations of e
single series (e
freedom). Acco
saphe in our lop

((log da

This rather unus

Before we a
is another nec
slightly on the
well as on the
power spectra fo
expected to have
of estimates, w
adjacent spectru
ratio, and this i
different total nu

DETAILS OF THE CROSS-CEPSTRUM APPROACH

At a single frequency two numbers are required to describe a cross spectrum. It is natural to introduce complex values by writing

$$(\text{cospectrum}) = \sqrt{-1}(\text{quadrature spectrum})$$

$$= (\text{magnitude or radius})e^{\sqrt{-1}(\text{phase})}$$

Here the cospectrum refers to an apparently common variation of an in-phase character, whereas the quadrature spectrum refers to apparently common variation that is 90° out of phase (= in quadrature); the cross-spectrum magnitude or radius expresses the apparently common variation after it has been adjusted to a maximum by applying the corresponding phase shift to the frequency constituents of one series.

CROSS CEPS

The cross
records, each wit
Figure 30, which
peak is about 10
echoes is illustra
records with ech
Had this mistin

The cross cepstrum can be written similarly as

$$\begin{aligned} (\text{cocepstrum}) + \sqrt{-1}(\text{quadrature cepstrum}) \\ = (\text{gamplitude or darius})e^{\sqrt{-1}(\text{saphe})}. \end{aligned}$$

For the present purposes this, the *lopar*, form seems most appropriate.

For a first attack on the analysis of two-receiver data, it may seem appropriate to concentrate on the darius as a function of quefrency. Another choice would be to make a lopar plot of the cross cepstrum (with quefrency as parameter) and look for peaks near saphes of zero and π (since these peaks are most clearly expected theoretically). In following up this alternative, we must be conscious that the sampling fluctuations of estimated darii are like those of spectrum estimates for single series (except for a doubling of the number of degrees of freedom). Accordingly, we should do well to combine *log* darius with saphe in our lopar plots, whose rectangular coordinates are thus

$$((\log \text{darius}) \cdot \cos (\text{saphe}), (\log \text{darius}) \cdot \sin (\text{saphe})).$$

This rather unusual plot seems to be quite effective.

Before we analyze seismic records by this approach, however, there is another necessary step. The $P-pP$ -delay is well known to depend slightly on the source-seismograph separation (epicentral distance) as well as on the depth of the source. Thus ripples in the liftered log power spectra for two stations at different epicentral distances will be expected to have slightly different quefrequencies (when expressed in terms of estimates, we have only to make the frequency steps between adjacent spectrum estimates of the two spectra different in the same ratio, and this is the natural consequence of calculating appropriately different total numbers of autocovariances for the two series).

CROSS CEPSTRA: EXAMPLES

The cross cepstrum of two independent artificial white noise records, each with an echo having $\alpha = -0.5$, $\tau = 15.0$ sec is illustrated in Figure 30, which gives a plot of the *log* darius against quefrency. The peak is about 10 db above the background. Selection against unwanted echoes is illustrated in Figure 31, which relates to the same original records with echoes of the same size, one at 15.0 sec and one at 17.0 sec. Had this mistiming been foreseen (for example, when comparing

seismic records at different known epicentral distances), it could have been allowed for, as shown by Figure 32. Here the same two records have been used, but the first was analyzed by using 400 lags in the initial autocovariance and the second with 453. The expected quefrequencies are now both 0.375 of their respective maximum quefrequencies, and the peak in the cross cepstrum is again apparent.

Figure 33 shows the effect of differences in spectral character in the original series and their echoes. The same white noise series was used for both records, with a "green" echo involving a filter with coefficients (0.50, 0.00, 0.49) and a delay of 5 sec. The resulting series was then passed through the bandpass filter illustrated by Figure 8 and also through a quite different filter with two narrow passbands. The cross-cepstral peak is quite apparent in Figure 33.

PSEUDO-CROSS COVARIANCES?

It would clearly be possible to experiment with pseudo-cross covariances of various forms. We have felt it wise to understand pseudo-autocovariances better before doing so.

Figure 30. Log
each

6. MORE DETAILED INQUIRY

COMPLEX DEMODULATION

Although spectral techniques, involving second-degree operations, are now quite familiar, the apparently simpler first-degree Fourier techniques are less well known. One of these may be described as *complex demodulation* [6]. To demodulate a time series $F(t)$ at a frequency f_0 , we form two new series:

$$x(t) = F(t) \cos 2\pi f_0 t$$

$$y(t) = F(t) \sin 2\pi f_0 t.$$

These are passed through a low-pass filter (a smoothing process) and the results are regarded as the real and imaginary parts of a complex function of time. The effect when $F(t)$ is the cosinusoid $A \cos(f_1 t + \epsilon)$ is to produce the series

LOG CEPSTRUM
-1.5
-1.8
-2.1
-2.4
-2.7
-3.0
-3.3
-3.6
-3.9
-4.2
-4.5

Figure 31. Log
one
hun
of b

ould have
o records
gs in the
expected
maximum
ent.
ver in the
was used
efficients
was then
and also
the cross-

udo-cross
derstand

operations,
Fourier
cribed as
 $f(t)$ at a

) and the
complex
 $f_1 t + \epsilon$) is

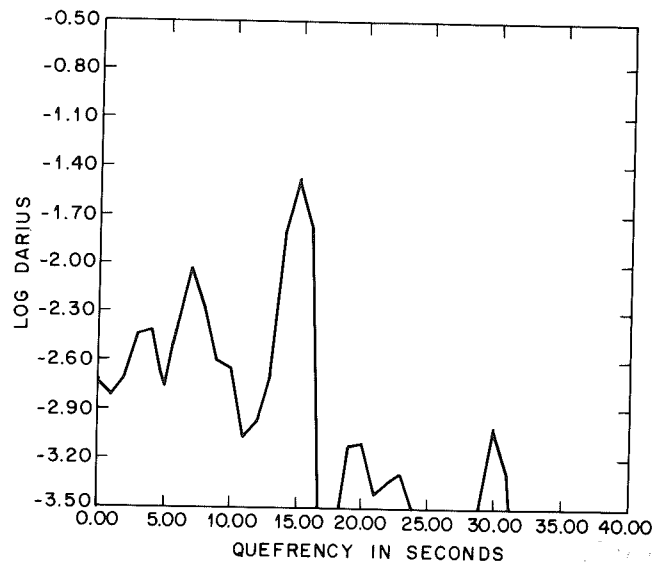


Figure 30. Log darius of the cross-cepstrum of two white noise samples each with an echo at 15 sec.

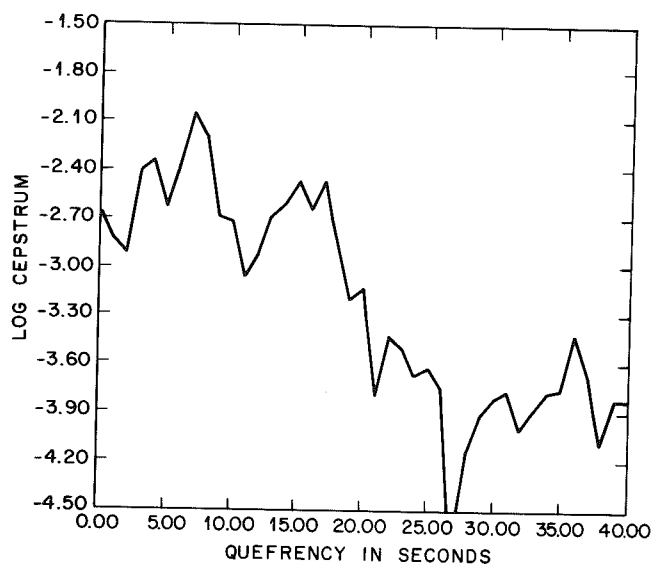


Figure 31. Log darius of the cross-cepstrum of two white noise records; one with a 15-sec echo, the other with a 17-sec echo. Four hundred lags were used for the autocovariance computation of both records.

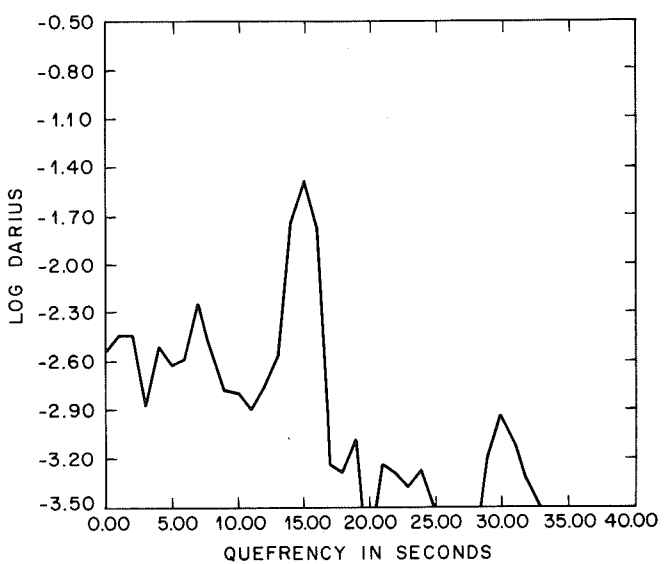


Figure 32. Log darius of the cross-cepstrum of the two noise records with different echoes. Four hundred lags were used in the autocovariance of the record with the 15-sec echo and 453 lags for the other.

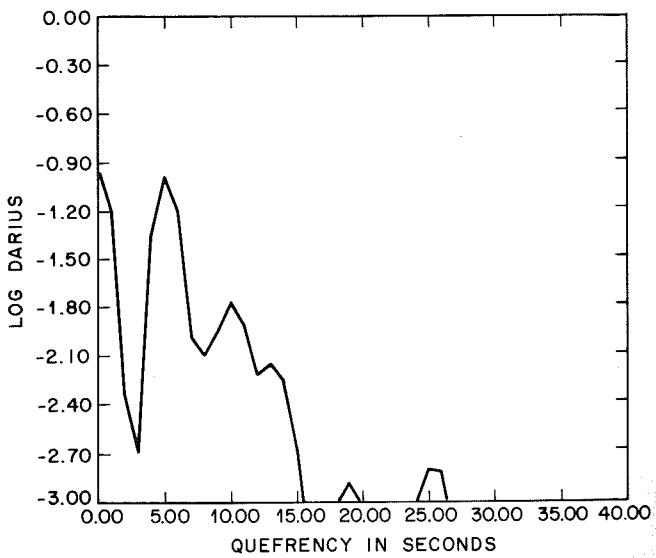


Figure 33. Log darius of the cross-cepstrum of a white noise plus green echo, filtered with two different filters having irregular transmission characteristics.

$$x(t) = \frac{1}{\sqrt{2}}(y_1(t) + y_2(t))$$

$$y(t) = \frac{1}{\sqrt{2}}(y_1(t) - y_2(t))$$

If f_1 is sufficiently large, the high-frequency component, $y_1(t)$, will be dominant. The instantaneous frequency component, $y_2(t)$, is a linear function of time, starting at $t = 0$. The constant term in $y_2(t)$ is the average amplitude and phase of the signal.

In an analysis of seismic signals, the complex dedomulating filter, $x(t)$, and saphe against the dedomulating quefrency, $y(t)$, have advantages as an analysis technique. It should prove more effective than the original method, since the information relative to the original signal is effectively preserved. It provides information about the frequency, hence the seismogram reflects the information relative to pP is expected to be more accurate. This can be envisaged as being greater than 0 or π .

SAPHE CRACKING

We have used the saphe technique to study stretches of saphe against the extended frequency range. Saphe cracking, has investigated the spectrum at each frequency. If we produce a plot of the log darius technique that all the values differ from the determined amplitudes, the slopes of saphe-vee and dedomulating quefrencies. The bandwidth of the saphe-vee ripple will show

$$x(t) = \frac{1}{2}A[\cos(2\pi(f_0+f_1)t + \epsilon) + \cos(2\pi(f_0-f_1)t - \epsilon)]$$

$$y(t) = \frac{1}{2}A[\sin(2\pi(f_0+f_1)t + \epsilon) + \sin(2\pi(f_0-f_1)t - \epsilon)].$$

If f_1 is sufficiently close to f_0 , the filter will effectively remove the high-frequency components with frequency (f_0+f_1) , leaving the low-frequency components with frequency (f_0-f_1) essentially undisturbed. The instantaneous phase, $\tan^{-1}(y(t)/x(t))$ of the low-frequency component, is a linear function of time with slope (f_0-f_1) and value $-\epsilon$ at $t = 0$. The complex time series thus provides information about amplitudes and phases in a narrow band of frequencies around f_0 .

In an alalysis context we can apply the analogous process of *complex dedomulation* to the liftered log spectrum, recording gamplitude and saphe against frequency for a narrow band of quefrequencies around a *dedomulating quefrency* τ_0 . This process may be expected to have two advantages as an echo detector over the use of the cepstrum: first, it should prove more powerful in detecting an echo whose amplitude relative to the original signal is strongly frequency-dependent, so that it is effectively present only over part of the total frequency range; second, it provides information on the saphe of the spectral ripple at zero frequency, hence on the sign of the reflection coefficient α . In seismology reflection at an air-ground interface such as that giving rise to pP is expected to give a negative reflection coefficient and situations can be envisaged in which α may become complex, giving saphes other than 0 or π .

SAPHE CRACKING

We have used this technique to a limited extent, looking for stretches of saphe that vary linearly with frequency over more or less extended frequency range. Our procedure, known to us as *saphe cracking*, has involved complex dedomulation of the liftered log spectrum at each of a sequence of dedomulating quefrequencies covering the same quefrency range as the cepstrum. At each of these quefrequencies we produce a plot of saphe against frequency by using a pre-edging technique that allows a point to appear on the plot only if its saphe value differs from those of the two adjacent points by less than a pre-determined amount. A transparent overlay can then be used to convert slopes of saphe-versus-frequency lines to quefrency differences. If the dedomulating quefrequencies are sufficiently close in terms of the bandwidth of the low-pass filter used in dedomulation, a particular ripple will show up on consecutive plots with the correct relative

slopes, and further confirmatory evidence can be obtained from the values of the gamplitude in the indicated frequency range (for the plots with smallest slope). It will be noted that if the gamplitude values for each quefrency are squared and averaged the resulting function of quefrency can be regarded as an estimate of the cepstrum using a window related to the dedomulation lifter.

REFERENCES

- [1] Blackman, R. B. and Tukey, J. W. (1959). *The Measurement of Power Spectra*. Dover, New York.
- [2] Bogert, B. P. (October, 1961). Seismic data collection, reduction, and digitization. *Bull. Seismological Soc. of Am.* **51**, 515-525.
- [3] Jeffreys, H. (1959). *The Earth* (Fourth Edition). University of Cambridge Press, Cambridge.
- [4] Richter, C. F. (1958). Elementary Seismology. W. H. Freeman, San Francisco.
- [5] Thirlaway, H. I. S. Depth of focus discrimination with the crust at first zone distances. *U.K.A.W.E. Special Report*.
- [6] Tukey, John W. (1961). Discussion, emphasizing the connection between analysis of variance and spectrum analysis. *Technometrics* **3**, 191-219.
- [7] Various authors (September, 1961). Papers on Spectrum Analysis. *Technometrics* **3**.

APPENDIX CALCULATIONS

The time series was recorded over a period of four years. A piece of paper was used to represent the paper registration. To get the registration must be done.

In 1961, the recorded information was subsequently hand digitized. Figures 34 and 35 show the digitized waveforms. They were sampled at a rate of 100 cps, running at a spacing of 1 mm. The folding frequency was 1.5 cps. The expected value was 1.5 cps.

Figure 34 shows the conclusion that the offered grid was surprising. The data showed that between

The figure shows the material as material. The series is similar to that at high frequencies. The digitization of the data shows the agreement between two spectra and appeared to be variations due to be interpolated by the equipment.

APPENDIX 1. INADEQUACIES OF HAND CALCULATION

The time series we have used have come either from a table of random normal deviates or from the output of a seismometer. Until three or four years ago, earthquake signals were almost always recorded on a piece of paper wrapped around a slowly rotating drum, so that the time series representing one day's record would appear as a series of lines on the paper. The recording speed for seismographs used for body-wave registration (so-called short-period seismographs) is generally 1 mm/sec. To get these records in a form suitable for analysis (or alalysis), they must be digitized by hand from suitable photographic enlargements.

In 1959 and 1960 we set up a seismometer at Chester, N.J., and recorded its output on magnetic tape. The earthquakes recorded were subsequently digitized electronically [2]. A measure of the quality of hand digitization, for a sample spacing of 0.1 mm, is shown on Figures 34 and 35. Figure 34 shows the spectra and the coherence of an electronically digitized earthquake record labeled CHP14 and a hand-digitized version CHP14H made from a playback of the first. The data were sampled at 10/sec and the playback was made onto a visual record running at 1 mm/sec. The hand digitization was made at 0.1 mm spacing between samples (10 samples/sec) so that in both cases the folding frequency is 5 cps. The introduction of irrelevant high-frequency energy is obvious, as is the lack of coherence above about 1.5 cps. The dashed line corresponding to $R^2 = 0.08$ corresponds to the expected value of R^2 for wholly uncorrelated time series.

Figure 35, which used as source data CHP13, leads to the same conclusions. Since CHP13 contained more high-frequency energy, it offered greater difficulty to the hand digitizer. Accordingly, it is not surprising that the coherence between it and CHP13H is poorer than that between CHP14 and CHP14H.

The fact that electronically digitized earthquake records were used as material for these comparisons is, in a sense, irrelevant. Any time series similar to these would have done as well. The lack of coherence at high frequencies is presumably due to noise introduced during hand digitization. However, coherence is an extremely sensitive measure of the agreement between two series. We have found low coherence between two electronic digitizations of the same event even though the spectra and the visual records derived from the two digitizations appeared identical. This seems to have been due to small speed variations of the order of 0.2 to 0.3% in the tape recorder which had to be interposed between the seismometer itself and the digitizing equipment.

Tables 1 an
chapter.

Column A

(1) = time
(2) = frequ
(3) = quefre
cepstrum

complex
dedomula

cross cepstr

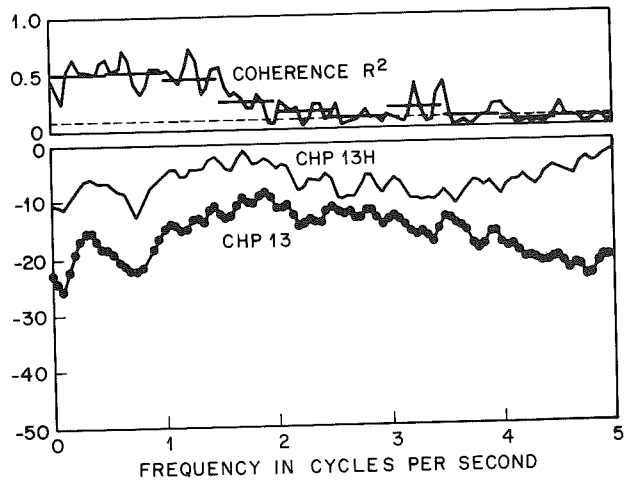


Figure 34. Log energy spectra and coherence R^2 for the seismic record CHP14 and its hand-digitized version CHP14H. The ordinate for the spectra is in decibels. The dashed line in the coherence plot is the expected coherence for unrelated signals.

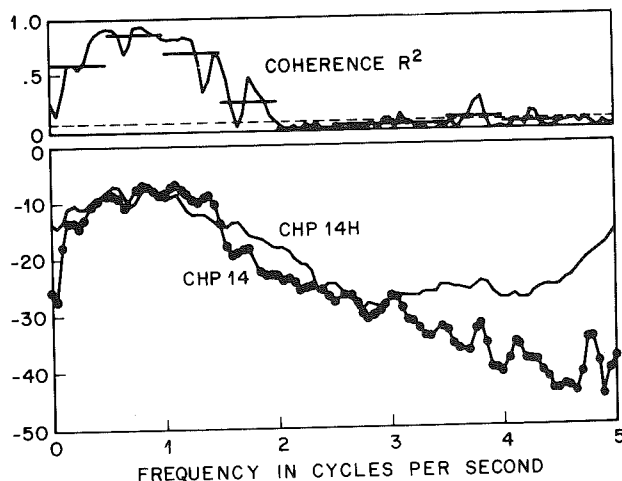


Figure 35. Log energy spectra and coherence R^2 for CHP13 and CHP13H.

APPENDIX 2. DEFINITIONS OF PARAPHRASED TERMS

Tables 1 and 2 list definitions of paraphrased and usual words in this chapter.

Table 1
**TERMS PARAPHRASED TO RECOGNIZE
 AN INTERCHANGE OF TIME AND FREQUENCY**

Column A	Column B	Definition
(1) = time (2) = frequency (3) = quefrency cepstrum	(1) = frequency (2) = time (3) = frequency spectrum	A dissection of the variance of (2) series into portions associated with various (3)'s.
complex dedemodulation	complex demodulation	A shifting of (3) in a (2) series by multiplication by sines, and by cosines, of a center (3), followed by smoothing (and sometimes decimation) of the two resulting (2) series, which can be regarded as the real and imaginary parts of a complex series. (Analogous to single-side-band modulation.)
cross cepstrum	cross spectrum	A dissection of the common variation of two (2) series, into portions associated with various (3)'s, which takes into account, and separates, both synchronized common variation (co-) and antisynchronized common variation (quadrature).

Table 1 (Cont'd)

TERMS PARAPHRASED TO RECOGNIZE
AN INTERCHANGE OF TIME AND FREQUENCY

Column A	Column B	Definition	TERMS PARAPHRASED TO RECOGNIZE AN INTERCHANGE OF TIME AND FREQUENCY	Used With Column A
liftering	filtering	A transformation of one (2) series into another which (a) obeys the superposition rule (is additive) and (b) is invariant under changes of (2) origin. (Conditions may be relaxed in other contexts.)		
lifter	filter	A device, formula, or process for making such a transformation.		alanysis
long-pass lifter	high-pass filter	One which passes more rapidly (2) varying components more readily.		darius
short-pass lifter	low-pass filter	One which passes less rapidly varying (2) components more readily.		gamplitude
quefrency	frequency	The number of cycles of a (2) series per unit (2).		lopar
rahmonic	harmonic	One of the high (3) (3) components generated from a sinusoidal component of a (2) series by a nonlinear process applied to the (2) series; or any equivalent (2) function.		saphe
repiod	period	The amount of (2) required for one cycle of a (2) series.		

Table 2
**TERMS PARAPHRASED AS REMINDERS THAT TIME AND FREQUENCY ARE
INTERCHANGED FROM TRADITIONAL USE**

Used With Column A	Used With Column B	Definition
alanysis	analysis	Procedure of summarizing, looking at, or dissecting data.
darius	radius	Modulus of complex number
gamnitude	magnitude	Modulus of complex number
lopar	polar	Plot or coordinates in terms of modulus and angle
saphe	phase	Angular displacement between a sinusoidal oscillation and a reference cosinusoid of the same (3) [the latter may be defined by an origin (2)].

THE
COLLECTED WORKS
OF
JOHN W. TUKEY

Volume I
TIME SERIES: 1949 - 1964

Edited by
David R. Brillinger
University of California, Berkeley

Charles J. Stone

Paul A. Tukey



WADSWORTH ADVANCED BOOKS & SOFTWARE
Belmont, California

ISBN 0-534-03303-2

© Copyright 1984 by Bell Telephone Laboratories Incorporated, Murray Hill, New Jersey.

All rights reserved. No part of this book may be reproduced or transmitted in any form or by any means, electronic or mechanical, including photocopying, recording, or any information storage and retrieval system, without the prior written permission of the publisher, Wadsworth Advanced Books & Software, 10 Davis Drive, Belmont, California 94002.

This book is a publishing project of Wadsworth Advanced Books & Software division of Wadsworth, Inc.

Library of Congress Cataloging in Publication Data

Tukey, John Wilder, 1915-

The collected works of John W. Tukey.

(The Wadsworth statistics/probability series)

Bibliography: p.

Includes index.

Contents: v. 1. Time series: 1949-1964.

1. Mathematical statistics--Collected works. 2. Time-series analysis--Collected works. 3. Tukey, John Wilder, 1915- --Bibliography. I. Title. II. Series.

QA276.A12T85 1984 519.5 84-15277

ISBN 0-534-03303-2 (v. 1)

Printed in the United States of America

1 2 3 4 5 6 7 8 9 10—88 87 86 85 84

The text for the book was processed at AT&T Bell Laboratories on a VAX 11/780 computer running the UNIX* operating system and troff/mm software driving an APS-5 phototypesetter. The font is Palatino.

*UNIX is a trademark of AT&T Bell Laboratories, Incorporated.